DYNAMIC SOLUBILITY OF PRESSURISED HELIUM GAS IN LIQUID PROPELLANT IN CLOSED STORAGE TANKS

K. Jokela[(1)], F. Valencia i Bel[(2)], I. Kälsch[(2)]

[(1)] European Space Agency, Materials Physics and Chemistry Section, Postbus 299, 2200 AG Noordwijk ZH, The Netherlands, Kristiina.Jokela@esa.int:
[(2)] European Space Agency, Propulsion Engineering Section, Postbus 299, 2200 AG Noordwijk ZH, The Netherlands, Ferran.Bel.Valencia@esa.int, Ingo.Kaelsch@esa.int

ABSTRACT

Up to now the solubility limits of most pressurant-propellant combinations have been identified, but the mechanism describing the solubility in function of time in closed propellant tanks has been without definite characterization. The solubility of a pressurised gas into liquid propellant creates pressure decay in a closed propellant tank after pressurisation. This paper presents the theory of dynamic gas solubility and its applications to current space programs. The parameters and variance of the dynamic solubility have been extracted from measured pressure decay data from the 4 ESA Cluster spacecraft and a number of American spacecrafts and implemented to predict the pressure decay in liquid MMH- and MON- propellant tanks of the ESA MSG and Rosetta spacecraft.

NOMENCLATURE

D_{AB}	mass diffusivity pressurant-propellant, m^2/s.
C_A	concentration of pressurant dissolved in the propellant, kg/m^3.
P	pressure, bar.
y	y-axis of the propellant tank defined as the depth of the tank, m.
K_g	mass convection coefficient, mole m^2 bar/h.
T	temperature, K.
R	gas law constant, $8.314510 * 10^{-5}$ bar m^3/moleK
T	time, h.
H	Henry's law constant, bar.
x_g	molar fraction of dissolved gas.
N	number of moles
M	mass, kg.
A_{g-l}	liquid-gas interface area.
V	volume, m^3.
$\overline{X}$	average value
$t_{n-1,95\%}$	t of student for n-1 samples and a level of confidence of 95%.
Z	compressibility factor.
Λ	saturation level.
E, F	empirical parameters (see eq.8)

MMH	Monomethylhydrazine
NTO	Nitrogen tetroxide
MON-1	Mixed Oxides of Nitrogen with 1% by weight of NO.
He	Helium gas.
N_2	Nitrogen gas.
S/C	spacecraft

Subscripts

dis	dissolved
sat	saturation
s	solvent
tot	total
FILL	Immediately after the pressurisation, t=0.
g	pressurant gas
AB	concerning binary diffusion
Ull	ullage

1 INTRODUCTION

Up to now the solubility limits of most pressurant-propellants combinations have been identified (see [2]), but the limits for the mechanism describing the solubility as a function of time are still not definitely explained. Solubility of a gaseous pressurant into liquid propellant creates a pressure decay in the closed propellant tank after pressurisation. By knowing the speed of the pressure decay, it would be possible to compute filling pressures that would then drop to the desired pressure at launch. Predicting the pressure drop would eliminate the need to re-pressurise, a hazardous operation requiring specific safety provisions, before launch.

This approach to predict the solubility of gaseous pressurant in liquid propellants in function of time under closed storage conditions is based on the theory of P.J. Knowles on helium adsorption [4].

It is recognized that the Knowles theory cannot fully cover the phenomena of dynamic pressure decay, especially the effect of temperature variations. The application of Fick's law for diffusion is seen as an improvement in order to model effects of variations in temperature and vibrations to the rate of solubility.

2 THEORY OF SOLUBILITY: LIMITS AND DYNAMICS

2.1 Solubility limit

Henry's law states that the concentration of the gas in the liquid phase is proportional to the partial pressure of the dissolved gas. Henry's law is expressed in eq.1.

$$P_g = x_g \cdot H = \frac{n_g}{n_s} \cdot H \qquad (1)$$

The variation of the partial pressure of a gas is never completely linear with variation of mole fraction x_g of gas in the liquid phase, especially when it is considered over the whole of the concentration range from $x_g = 0$ to $x_g = 1$. Nevertheless, for low concentration of gas in liquid phase, when $x_g < 0.01$, the variation of experimental errors usually fit a linear relation within experimental error [1].

The solubility varies also as a function of temperature. Nevertheless, this feature is dependent on the interactions between the molecules in the liquid phase and therefore it is a gas-liquid specific parameter that is normally determined empirically. The solubility limits of He(g) and N_2(g) for propellants can be found in [2] and [3].

Chang and Gocken [2] measured the mass fraction of dissolved helium in liquid NTO and MMH. They presented the following correlations as a function of temperature and pressure, for NTO:

$$\frac{m_{He,dis}}{m_{NTO}} = 10^6 \cdot 10^{(-153/T+2.8194)} \cdot P_{He} \cdot \Lambda/1.013 \qquad (2)$$

and for the mass fraction of the dissolved helium into liquid MMH:

$$\frac{m_{He,dis}}{m_{MMH}} = 10^6 \cdot 10^{(-393/T+1.6586)} \cdot P_{He} \cdot \Lambda/1.013 \qquad (3)$$

When the liquid propellant has adsorbed the maximum amount of gas Λ equals 1. When the liquid doesn't contain any dissolved helium and the liquid is exposed to helium Λ equals 0. Eq.2 and eq.3 are valid for a range between 0°C and 30°C.

2.2 Dynamic solubility

A simplified analytical technique has been developed for simulating the adsorption phenomena under closed storage conditions. The model has been used to evaluate the propellant conditions for Apollo missions [4]. Mass convection analogy, Dalton's law on partial pressures and Henry's law for liquid solubility were used in the development of the formulation. It was assumed that:

- The system is closed: no leakage or flow exist
- All diffusion is normal to the gas/liquid interface
- Propellant vapour pressure is constant
- Constant temperature

Hence:

$$\frac{P - P_{sat}}{P_{FILL} - P_{sat}} = e^{\left(\frac{-K_g A_{g-l} Z_g RT\, t}{V_{ull}}\right)} \qquad (4)$$

Where P in this case is the pressure in the ullage volume at any instant of time.

3 DYNAMIC SOLUBILITY LIMITS FROM MEASURED DATA

Fig. 1, Fig.2 and Fig.3 present the measured data points and the calculated curves of the helium solubility in liquid NTO and MON-1 in the closed propellant tanks in different spacecraft. The measured points were standardised taking into account the changes in vapour pressure, liquid density and gas density in function of temperature to a chosen temperature (22ºC and 21ºC, see figures) from their original values. The calculated pressure decay curve, corresponding to measured values from a S/C, was made by best-fit adjustment of K_g in eq. 4 to the measured values. According to the eq. 4 the dynamic pressure drop depends on temperature T, initial pressure P_0, saturation pressure P_s, ullage volume V_{ull} and ullage volume fraction V_{ull} - %, The value of K_g can be seen in the key of the graphs. Saturation pressure P_s depends on the initial saturation level of the propellant Λ and the filling pressure.

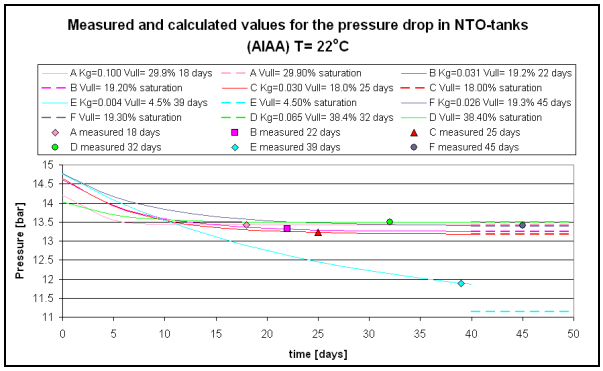

Fig. 1. Variation of tank pressure in function of time for He - pressurised NTO tanks of different American spacecraft. Measured points were standardised at 22ºC and pressure decay calculated. V_{tot} varies between 0.2107 - 0.3704 m^3. [6]

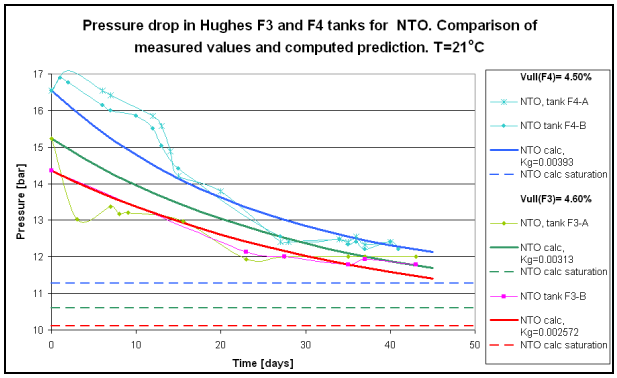

Fig. 2. Variation of the tank pressure in function of time for the Hughes F3 and F4 He - pressurised NTO tanks. Measured points were standardised at 21ºC and pressure decay calculated. V_{tot} = 0.3075 m^3. [6]

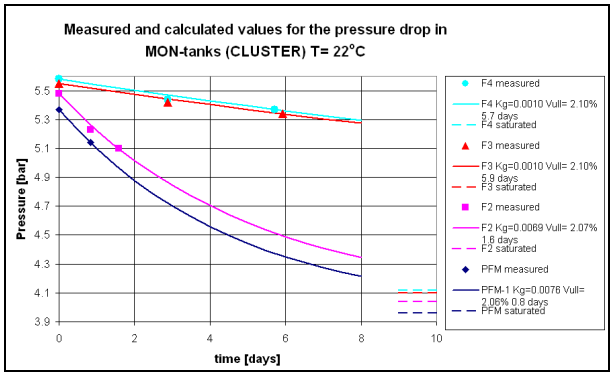

Fig. 3. Variation of the tank pressure in function of time for Cluster He - pressurised MON-1tanks. Measured values were standardised at 22ºC. V_{tot} = 0.297 m^3.

Table 1 presents a summary of the K_g values in figures 1, 2 and 3 for Helium solubility in MON-1 and NTO.

Table 1 Variation of the mass convection coefficient K_g for He –solubility in liquid NTO and MON-1.

Source of Data	Propellant	Ullage Volume Fraction [%]	Initial Pressure [bar]	K_g [mol m^2 bar/h]	Recording Period [days]
Small Ullage Volume Fraction (<10%)					
Cluster (5)	MON-1	2.06	3.96	0.0076	0.8
	MON-1	2.07	4.04	0.0069	1.6
	MON-1	2.10	4.10	0.0010	5.9
	MON-1	2.10	4.10	0.0010	5.7
AIAA (6)	NTO	4.50	12.95	0.0040	39.0
Hughes (6)	NTO	4.60	13.11	0.0039	0-40
	NTO	4.50	13.26	0.0026	0-40
Medium Ullage Volume fraction (>10%, <25%)					
AIAA (6)	NTO	18.0	13.18	0.030	25
	NTO	19.2	13.31	0.031	22
Large UllageVolume Fraction (>25%)					
AIAA (6)	NTO	29.9	13.40	0.100	18
	NTO	38.4	13.96	0.065	32

As in the case of NTO/MON the figures 4, 5 and 6 present the measured data points standardised (to 21ºC and 22ºC) and the calculated pressure decay curves of the helium solubility in liquid MMH with the best-fit molar convection coefficients K_g.

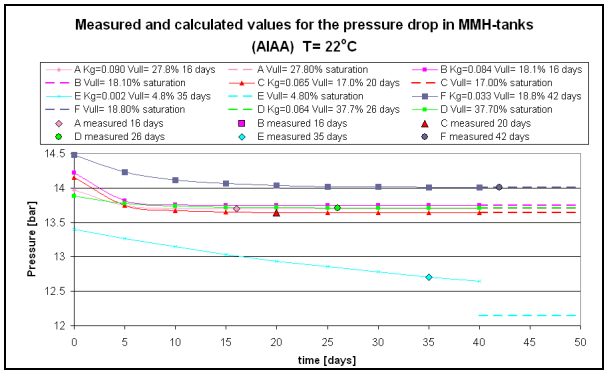

Fig. 4. Variation of the tank pressure in function of time for He - pressurised MMH tanks of different American spacecraft. Measured points were standardised at 22ºC and pressure decay calculated. V_{tot} varies between 0.2107 - 0.3704 m^3.

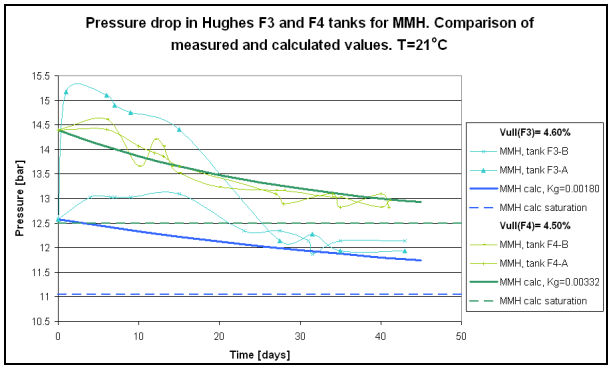

Fig. 5. Variation of the tank pressure in function of time for Hughes F3 and F4 He - pressurised MMH tanks. Measured points were standardised at 21ºC and pressure decay calculated. V_{tot} = 0.3075 m^3.

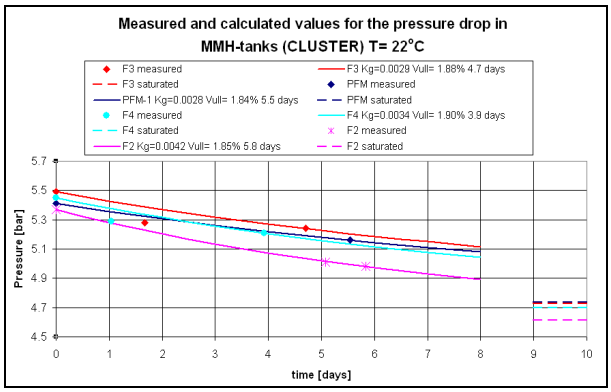

Fig. 6. Variation of the pressure with time for He - pressurised MMH tanks of Cluster. Measured values were standardised at 22ºC. V_{tot} = 0.297 m^3.

Table 2 presents a summary of the Kg values in figures 1, 2, 3 and 4 for Helium solubility in MMH.

Table 2 Variation of the mass convection coefficient K_g for He –solubility in liquid MMH.

Source of Data	Ullage Volume Fraction [%]	Initial Pressure [bar]	K_g [mol m^2 bar/h]	Recording Period [days]
Small Ullage Volume Fraction (<10%)				
Cluster (5)	1.84	5.4	0.0028	5.5
	1.85	5.4	0.0042	5.8
	1.88	5.5	0.0029	4.7
	1.90	5.5	0.0034	3.9
Hughes (6)	4.5	14.4	0.00332	0-40
	4.6	12.6	0.0018	0-40
AIAA (6)	4.8	12.5	0.002	35
Medium Ullage Volume fraction (10% -25%)				
AIAA (6)	17	13.4	0.065	20
	18	13.5	0.084	16
Large UllageVolume Fraction (>25%)				
AIAA (6)	27.8	13.5	0.090	16
	37.7	13.6	0.064	26

It can be noticed in Table 1 and Table 2 that K_g varies to some extent in function of ullage volume fraction: the smaller ullage volume fraction the smaller the K_g hence the pressure decay occurs at slower rate compared to the tanks with larger ullage volume fractions. Probably the initial pressure and the propellant / gas interface area to some extent influence K_g, but the exact evaluation cannot be made due to the lack of data. It is assumed that the total volume of the tank does not have a significant effect in the variance of K_g in the range of measured data of 0.21m^3 to 0.37m^3. It should be also taken into account that the data plotted in figures 1 and 4 had only two measured points per s/c, which is not enough for giving a reliable estimation about the speed of solubility.

4 DYNAMIC SOLUBILITY PREDICTIONS FOR MSG AND ROSETTA

Due to lack of measured data, it was impossible to make reliable and accurate predictions for the pressure decay. Yet, a successful evaluation was made for predicting pressure decay for the MMH and MON-1 tanks of MSG (Fig. 7).

4.1. MSG

The MSG pressure decay was evaluated at a constant temperature 21ºC. Upper and lower limits for the K_g were extracted from the available data as follows: for MMH K_g(max) = 0.0255 and K_g(min) = 0.0034; for MON-1 K_g(max) = 0.0093 and K_g(min) = 0.0036. K_g was constant.

In order to have the launch pressures in the propellant tanks not exceeding 13 bar (at 25ºC) and the pressure difference between the MMH and MON tanks less than 1 bar, it was decided to pressurise the MON-1 tanks to 15.65 bar and the MMH tanks to 13.34 bar at 21ºC. The prediction gave upper and lower limits for the possible tank pressures. (See Fig. 7)

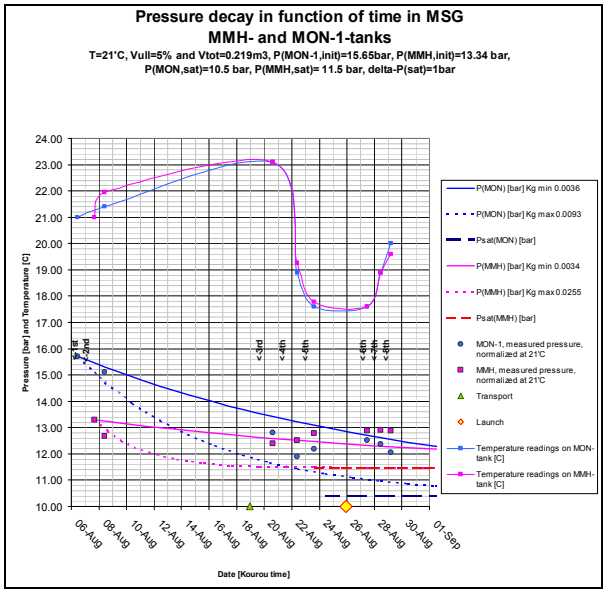

Fig. 7. Predicted pressure evolution and the measured pressure. The pressure predictions were established for a constant 21^{o}C temperature. The measured values were taken at different temperatures and then normalised to 21^{o}C taking into account the changes in density, vapour pressure and ideal gas expansion/contraction.

It can be summarised that when the temperature increases: 1) the density of the liquid propellant decreases, which leads to a smaller ullage volume and compression of the ullage volume gases, $P_{tot}\uparrow$; 2) the vapour pressure of the propellants increases, $P_{tot}\uparrow$; 3) the solubility increases, which increases the dynamic solubility, $P_{tot}\downarrow$. In the tank with a small ullage volume fraction, like MSG, the effects of 1 and 3 are accentuated.

It has been computed from the MSG data that lowering the temperature releases some helium out of solution, and increasing the temperature increases the amount of dissolved helium.

The gas gets into solution at the liquid-gas interface. It is supposed that the liquid at the interface is fully saturated with helium to a certain depth from the surface. The saturating mass fraction of helium depends on the temperature (see eq. 2 and 3). As the solubility of helium in liquid propellants increases with temperature, a drop in temperature means that capacity

for the liquid to adsorb helium diminishes and the excess of helium, which was dissolved at higher temperature, escapes from the liquid.

Another remark can be made on the influence of vibrations. It is assumed that when the tanks are still, the dissolved gas is going towards the bottom of the tank by diffusion, in other words, by difference of concentration of pressurant in the propellant between the gas-liquid interface (that is fully saturated) and the bottom of the tank (partially saturated). When the spacecraft is moved, the stratified layers of propellant at different saturation level are disturbed. Also temperature changes of the propellant tank can, pending on source and location, cause convective flow / movement of the propellant. Thereby propellant at different saturation level becomes mixed and relatively unsaturated propellant exposed to the pressurant gas. This may enhance the saturation rate considerably.

The time to reach complete saturation of the propellant depends on the amount of gas dissolved in the propellant before and during tank pressurisation for flight. For MSG it was estimated that more than 20 days would be required to reach full saturation. It could be also interpreted from the measured data that the dynamic solubility increases when the temperature is augmented and therefore the mass of helium in the ullage decays faster (which corresponds to the faster pressure decay in Fig. 7). On the other hand, when the tanks are cooled down the dissolution of gas seems to stop. Actually, dissolved helium gets out from the over-saturated propellant close to and at the gas-liquid interface, thereby increasing the amount of helium in the gas phase.

The MSG data provided a valuable input to the helium solubility database and prediction tool for the benefit of future ESA satellites.

4.2. ROSETTA

A prediction of pressure decay (similar to that for MSG) was made for the MMH and MON-1 tanks of ROSETTA. Yet, when the large ullage volumes of the ROSETTA tanks were pressurised, the temperature rose over 30ºC, which accelerated the rate of helium dissolution. Therefore, plenty of helium went into solution during the period of tank pressurisation and it was unknown how much helium was dissolved in the liquid in the beginning. When the temperature of the tanks decayed to ambient level, the excess of helium came out of solution and establishing a useful prediction was impossible.

When the tank pressures finally stabilised (the propellant became fully saturated with helium), it was possible to model the pressure decay with eq. 4 (e.g. model proposed by P.J. Knowles, with a constant K_g). The results are shown in Fig. 8.

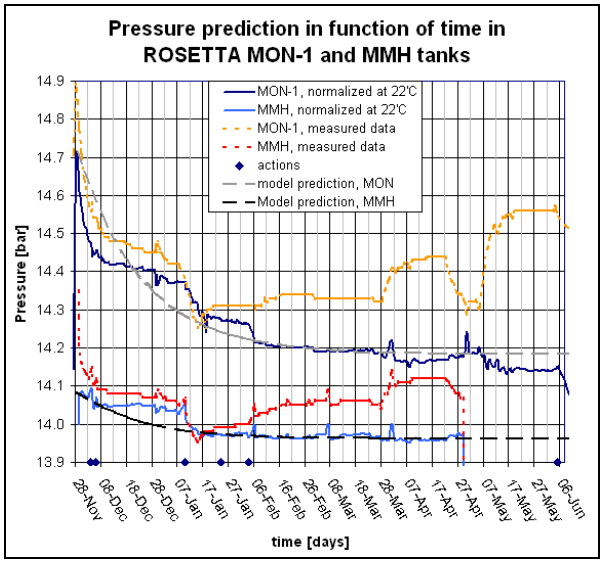

Fig. 8. ROSETTA: Measured tank pressures (dashed line) and standardised pressures at 22ºC (The changes in density, vapour pressure and ideal gas expansion/contraction were taken into account for the standardisation.). Pressure decay computed with the best-fit method of eq. 4.

The characteristic value of K_g for ROSETTA (Fig 8) was different from the values obtained from Hughes and MSG. From the assessment of the data it can be concluded that the temperature fluctuation has an important role in the dynamic solubility process. The movements of the S/C were having also some effect on the solubility.

From the results obtained from ROSETTA, it appeared that it was necessary to model the effect of fluctuating temperature and the effect of the dimensions of the system in the rate of pressure decay in the propellant tanks.

4.3. Update to Knowles theory. Fick's Law.

Reviewing the results obtained with Knowles approach (eq. 4) and applied to MSG and ROSETTA, one can conclude that K_g is not constant. Therefore, a formulation for a variable K_g was established by using Fick's law of diffusion, since it appeared that the rate at which the pressurant gets into solution depends on the pressurant (helium) concentration gradient in the liquid propellant.

Fick's law is written as:

$$N''_A = A_{g-l} \cdot \left(-D_{AB} \cdot \frac{\partial C_A}{\partial y} \right) \qquad (5)$$

Following the methodology and notation used in section 2.2 (originally from [4]) and applying eq. 5 K_g becomes:

$$K_g = \frac{-D_{AB} \cdot \left(\frac{\partial C_A}{\partial y}\right)_{y=0}}{P - P_S} \quad (6)$$

Where D_{AB} is dependent on the level of "shaking" of the liquid and temperature (see eq. 7 and eq. 8).

$$D_{AB} = D_{AB,static} + D_{AB,turbulent} \quad (7)$$

$$D_{AB} = D_{AB,static} = E \cdot \exp\left(-\frac{F}{T}\right) \quad (8)$$

If the time of "shaking" is sufficiently low compared to the total time needed to saturate the propellant (<5%), $D_{AB,turbulent}$ can be ignored (and set to zero). Based on experience from the measured data, the amount of pressurant dissolved during this period is relatively small compared to the total amount of pressurant gas dissolved. In addition, reliable models for the prediction of $D_{AB,turbulent}$ are not yet established [8]. More input data is required to predict $D_{AB,turbulent}$. A proper characterisation of the disturbances during the "shaking" is needed (frequency and amplitude).

This updated set of equations (namely eq. 6, 7 and 8) takes changes in temperature into account and therefore is able to model pressure variations and change of solubility rate due to temperature changes in the system. The methodology has been applied to the available data on NTO/MMH tanks of Rosetta, MSG, Hughes, Cluster, Cluster II. The results obtained are summarised in Table 3.

Table 3 Results obtained using Fick's law.
E and F correspond to the constants from eq. 8.

Spacecraft		MON		MMH	
		D_{AB} (m^2/s)		D_{AB} (m^2/s)	
		E	F	E	F
Rosetta		4.98E-07	651.9	3.90E-05	2100
MSG		2.50E-07	651.9	3.40E-05	2100
Hughes	F3-A	2.66E-06	651.9	-	-
	F3-B	2.35E-06	651.9	1.12E-04	2100
	F4-A	2.82E-07	651.9	1.04E-04	2100
	F4-B	2.82E-07	651.9	4.88E-04	2100
Cluster	PFM	3.04E-05	651.9	8.00E-06	2100
	F2	3.54E-05	651.9	1.64E-04	2100
	F3	4.38E-07	651.9	5.60E-05	2100
	F4	1.57E-07	651.9	3.20E-04	2100
Cluster II	F6	2.35E-07	651.9	1.34E-04	2100
	F7	3.13E-07	651.9	1.22E-04	2100

Table 3 shows a large scatter in the calculated data for the constant E. For MON, 8 out of 12 data points seem to be in good agreement, while for MMH the scatter is larger and a good agreement is difficult to identify. However, based on the experiments that show a good agreement (in Table 3) an average value and a deviation have been computed. Using a level of confidence of 95%, an upper and a lower limit could be defined. Both limits are summarised in eq. 9.

$$\overline{X} - t_{n-1,95\%} \cdot S \geq \overline{X} \geq \overline{X} + t_{n-1,95\%} \quad (9)$$

By using eq. 9, a fastest and a slowest pressure decay was obtained, the maximum deviations observed for all cases and for ROSETTA (where a more intensive follow-up was done) are shown in Table 4.

Table 4. Maximum pressure deviations observed

	All cases	ROSETTA
MON/He	± 0.5 bar	± 0.1 bar
MMH/He	± 0.2 bar	± 0.04 bar

In addition, [8] presented results from experiments on diffusion of pressurant in different propellants. The results are shown in Table 5.

Table 5. Comparison of diffusion rates for different propellant-pressurant combinations.

D_{AB} at 25°C (m^2/s)		
	Averaged results	American [8]
MON/He	$3.61 \cdot 10^{-8}$	$3.52 \cdot 10^{-8}$
MMH/He	$8.83 \cdot 10^{-8}$	-
Hydrazine/He	-	$6.44 \cdot 10^{-8}$
NTO/N_2	-	$6.90 \cdot 10^{-9}$
Hydrazine/N_2	-	$1.60 \cdot 10^{-8}$

As seen in the data in Table 5 there is a good agreement for calculated averaged MON/He systems values with the values found in [8].

In light of the data available, it has been observed that diffusion varies with the density of the liquid. The higher the density, the lower is the diffusion, in other words, it seems that for low-density propellants less time is required to reach the saturation level.

Fig. 9 and Fig. 10 show the comparison between the actual measured pressure and modelled pressure limits computed with the new model (eq. 6, 7 and 8) for ROSETTA's MON and MMH tanks.

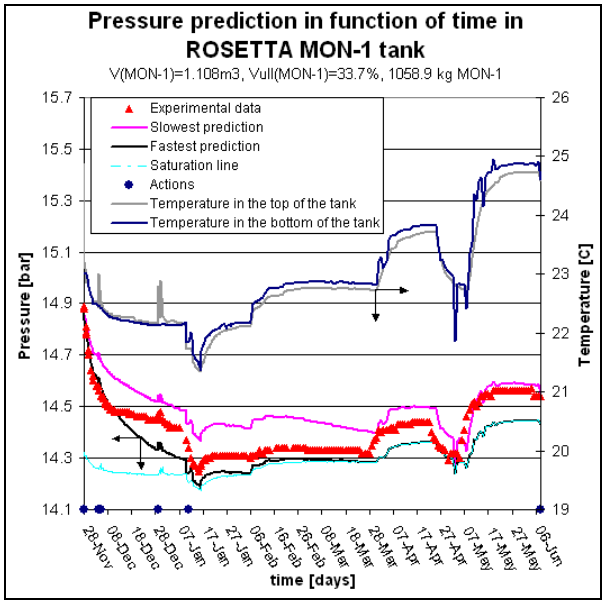

Fig. 9. ROSETTA: Comparison of the measured (experimental) tank pressure evolution of MON-1 tanks and the pressure decay limits (fastest and slowest predictions) computed with the up-dated model.

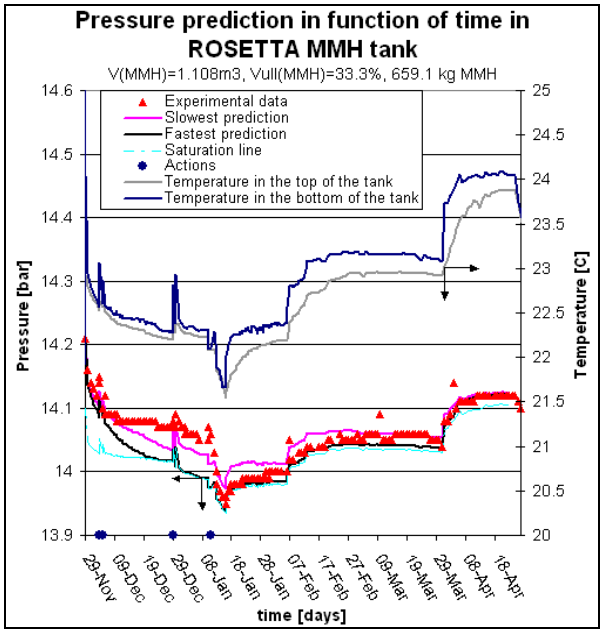

Fig. 10. ROSETTA: Comparison of the measured (experimental) tank pressure evolution of MMH tanks and the pressure decay limits (fastest and slowest predictions) computed with the up-dated model.

The model is able to model the temperature variations in the time. Fig. 9 and Fig. 10 show that when the propellant is fully saturated the pressure variations are due to temperature changes in the tank.

5 CONCLUSIONS

It has been noticed that already during the pressurisation of the tanks an imposing amount of gas is dissolved in the propellant. This amount of dissolved pressurant gas seems to depend on the actual pressurisation process and is difficult to evaluate. Nevertheless, there are approaches for estimating this amount of initially dissolved gas if sufficient data (temperatures, pressures) are available from the pressurisation process.

The mechanisms that characterise the pressure decays in the propellant tanks due to dissolution of the pressurant gas to the propellant after completion of the pressurisation process have been identified and modelled. The models proposed (Knowles and Fick's law) seem to cover the mechanisms sufficiently. In order to validate the model and to establish reliable future predictions, recordings / data from real S/C projects of propellant tank pressurisation to launch level and of subsequent actual pressure decay are needed as follows:

- Temperature in the liquid and the gas phase.
- Total pressure in the tank
- The compilation of the data should be more exhaustive, e.g. quasi-continuous recording during pressurisation for flight, at least 2 readings per day during the first week after pressurisation, and 1 reading per day afterwards.
- Description of any activities with the S/C that might cause disturbance of the propellant – pressurant gas interface, such as displacement of the S/C.

In light of the data available, it seems that for propellant tanks with small ullage volume fractions (<10 %) the Knowles approach [4] gives often-accurate enough results, as in the case of MSG. For larger ullage volume fractions, like on ROSETTA, the up-dated model with Fick's law is recommended to model the pressure decay.

6 REFERENCES

1. Solubility of Gases in Liquids, A Critical Evaluation of Gas/Liquid Systems in Theory and Practise, P G T Fogg and W Gerrard, John Wiley & Sons, 1991, page 287

2. Solubilities of Gases in Simplex and Complex Propellants, Chang, Gocken and Poston, Journal of Spacecraft and Rockets, Vol.6 No 10, pp. 1177, Oct 1969
3. USAF Propellant Handbook NTO/MON, Vol. II, Martin Marietta Corporation, AFRPL-TR-76-76, Feb. 1977
4. Helium Adsorption into Nitrogen Tetroxide (NTO) and Aerozine-50 (A-50), Philip J. Knowles, TRW Systems, Houston, Texas, J. Spacecraft Sep. 1972, vol. 9, no. 9.
5. Cluster Project, Propellant Tank Pressure Drop Due to the Saturation, I. Kaelsch, ESA/ESTEC/TEC-MPC, 1996
6. Loading Operations for Spacecraft Propulsion Subsystems, G.P. Purohit, H.O. Nordeng, AIAA-92-3065, 28th Joint Propulsion Conference and Exhibit, July 6-8 1992/Nashville.
7. CFD Corporation; CFD-ACE-GUI Modules Manual; May 2003.
8. Johnson, R.L.; Bhuta, P.G.; A study to analyze the permeation of high density gases and propellant vapours through single layer TEFLON or TEFLON structure materials and laminations; NASA Western Operations office, 07282-6032-R0-00 August 1969.